Chemistry of anthracene–acetylene oligomers. XVII. Synthesis, structure, and dynamic behavior of 1,8-anthrylene pentamers and hexamers with acetylene linkers†‡

Shinji Toyota,* Takahiro Kawakami, Risa Shinnishi, Rie Sugiki, Shinya Suzuki and Tetsuo Iwanaga

Received 19th June 2010, Accepted 10th August 2010
DOI: 10.1039/c0ob00290a

Three types of cyclic oligomers consisting of five or six 1,8-anthrylene units with acetylene linkers were synthesized by macrocyclization of the corresponding acyclic precursors with coupling reactions. DFT calculations at the M05/3-21G level revealed that the pentamers had a relatively rigid structure with strained alkyne carbons. Meanwhile, out of several possible conformers the hexamers preferred to take parallelogram-prism structures due to transannular π···π interactions, and conformational interconversions *via* rotation about the acetylene axes took place rapidly at room temperature. NMR spectra and electronic spectra are discussed on the basis of molecular structures. The enantiomers of the chiral hexamer with one diacetylene linker were resolved by chiral HPLC, and showed optical activity.

Introduction

We synthesized various types of oligomers consisting of anthracene and acetylene building units[1] as novel arylene–ethynylene oligomers in the field of π-conjugated compounds.[2,3] Those studies have shown that four 1,8-anthrylene units and four acetylene (or diacetylene) linkers could form cyclic structures **1–3** with negligible or small strains (Fig. 1).[4,5] Spectroscopic measurements have revealed that the structures, dynamic behavior, and properties of these cyclic tetramers are affected by the combination and position of the two kinds of linkers. For example, tetramers **1** and **2** undergo exchanges between two diamond-prism conformations, while tetramer **3** has a rigid and chiral framework. The cyclic structures are modified by changing the number of aromatic units, and as examples of such compounds, we recently reported cyclic trimer **4**[6] and dimer **5**.[7] The cyclic framework is significantly deformed in the former system due to geometrical requirements, while it is practically planar in the latter. These results demonstrate that molecular deformations in oligomer systems strongly depend on the number of building units, namely whether odd or even.

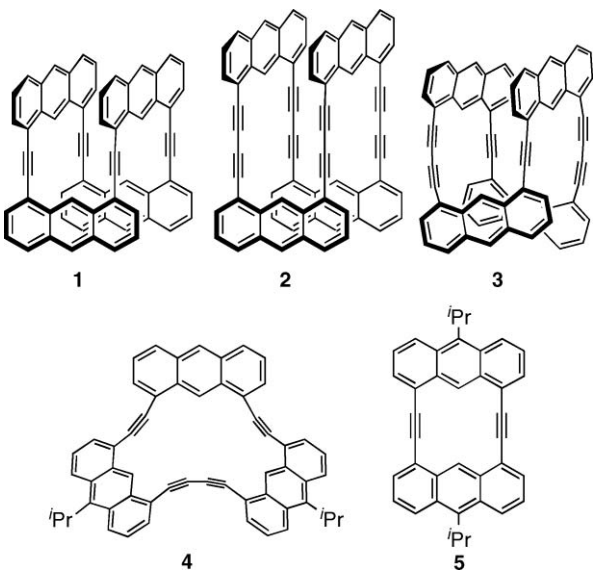

Fig. 1 1,8-Anthrylene oligomers with acetylene and diacetylene linkers.

Higher anthrylene–ethynylene oligomers are attractive target compounds not only to verify the above geometrical necessity but also to examine their flexibility and dynamic behavior[2,8] even though the construction of macrocyclic rings is not always easy from the viewpoint of entropy. This background has encouraged us to synthesize cyclic anthrylene–ethynylene pentamers and hexamers as odd and even number series macrocyclic oligomers, respectively (Fig. 2). In pentamer **6**, five 1,8-anthrylene units are connected by four acetylene linkers and one diacetylene linker to form a deformed framework. In contrast, hexamer **8** is highly symmetric with six acetylene linkers, and hexamer **7** has a chiral structure with one diacetylene linker incorporated. These hexamers are regarded as belt-shaped molecules consisting of π-system building units,[9] and their frameworks should be conformationally flexible in contrast to those of shape-persistent π-conjugated compounds.[3] Schlüter and coworkers recently proposed the molecular design of a macrocyclic scaffold with three 1,8-anthrylene and three *m*-terphenyl units to construct hexagonal two-dimensional polymers.[10] Compound **8** is regarded as an all-anthracene version of the hexagonal scaffold. We herein report the structure, properties, and dynamic behavior of these macrocyclic compounds based on spectroscopic data and DFT calculations. The resolution of the chiral hexamer is worthwhile because information on the chiroptical properties of such chiral belt-shaped molecules is limited.[11,12]

Department of Chemistry, Faculty of Science, Okayama University of Science, 1-1 Ridaicho, Kita-ku, Okayama 700-0005, Japan. E-mail: stoyo@chem.ous.ac.jp; Fax: +81-86-256-9457; Tel: +81-86-256-9457

† Part 16 of the series, see ref. 1.

‡ Electronic supplementary information (ESI) available: Analytical and spectroscopic data of some compounds, NMR charts of cyclic oligomers, and UV–vis and fluorescence spectra of cyclic and acyclic oligomers. See DOI: 10.1039/c0ob00290a

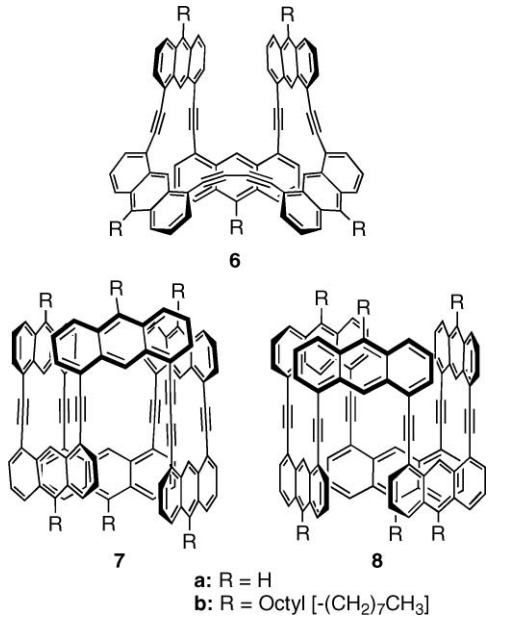

Fig. 2 Target 1,8-anthrylene macrocyclic oligomers: pentamer **6**, chiral hexamer **7**, and achiral hexamer **8**.

Results and discussion

Synthesis

Cyclic pentamers were synthesized according to Scheme 1. We initially synthesized cyclic pentamer **6a** that contained no alkyl groups. Pentamer **18a** was prepared by the Sonogashira coupling of **16a**[6] with 1,8-diiodoanthracene (**17a**).[13] After desilylation of **18a** with tetrabutylammonium fluoride (TBAF), the formed terminal alkyne was treated with copper reagents to promote Eglinton coupling.[14] Although the poorly soluble nature of the desired cyclized product hampered workup and purification procedures, we managed to obtain a pure sample of **6a** in 17% yield as a yellow solid. However, as this product was far from practical for further investigations, we introduced an octyl group at the 10-position of each anthracene ring to improve solubility. Dimer **16b** was prepared from 4,5-dichloro-9-anthrone (**9**)[15] in six steps in a conventional manner. The Sonogashira coupling of this dimer with **17b**[16] gave pentamer **18b** in 53% yield. In the series of syntheses of octyl-substituted derivatives, the yields of the Sonogashira coupling to form **15b** and **18b** were improved by the use of H_2 gas rather than N_2 gas, as reported previously.[17] Compound **18b** was cyclized in a similar manner to give **6b** as a yellow solid in 60% yield, and this product was reasonably soluble in chloroform.

Hexamers **7b** and **8b** were also synthesized from pentamer **18b** (Scheme 2). Compound **18b** was slowly desilylated with TBAF in dichloromethane, and partially desilylated product **19b** was obtained after chromatographic separation. The chain of this pentamer was extended by the Sonogashira coupling with **14b** to give **20b**. This precursor was similarly subjected to macrocyclization to give **7b** in 60% yield as a yellow solid. For the synthesis of achiral hexamer **8b**, compound **19b** was reacted with excess diiodoanthracene **17b** to give hexamer **21b**. This precursor was subjected to desilylation followed by macrocyclization by the Sonogashira coupling. The cyclized product was obtained as a yellow solid in low yield. All macrocyclic compounds gave molecular ion peaks at the calculated molecular weights by FAB mass spectroscopy: m/z 1024.31 (**6a**), 1584.94 (**6b**), 1897.13 (**7b**), and 1873.12 (**8b**).

NMR spectra

The NMR spectra of pentamers **6** at room temperature are consistent with the spectra of structures having C_s symmetry, where the plane of symmetry contains the midpoint of the diacetylene linker and the 9,10-C atoms in anthracene **C** at the opposite side (see Scheme 1 for symbols specifying anthracene units). For example, in the case of **6b**, five sets of ABC systems and three singlets (2 : 2 : 1 intensity) were observed in the aromatic region of the ^{1}H NMR spectrum [Fig. 3(a)] and six alkynic carbon signals were seen in the ^{13}C NMR spectrum. Some aromatic signals

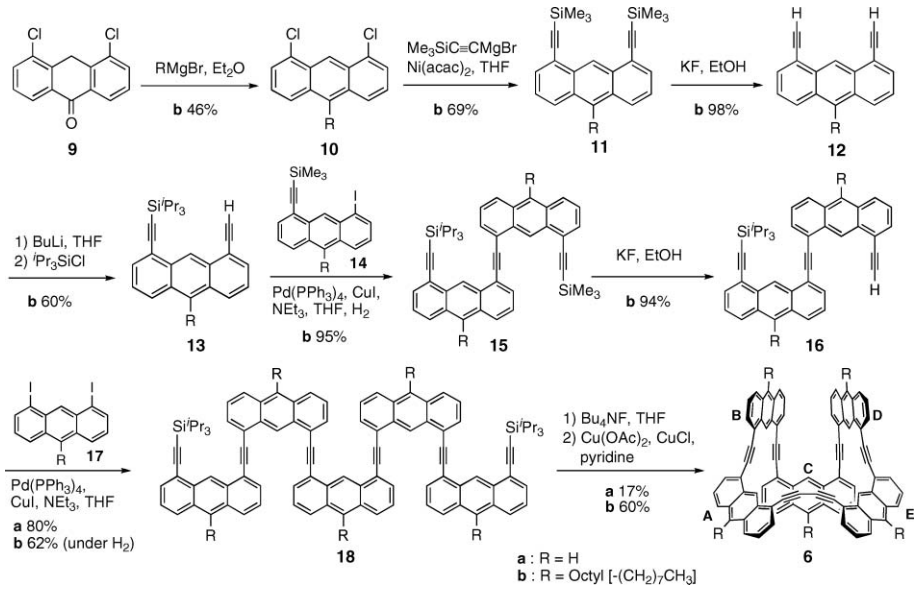

Scheme 1 Synthesis of acyclic precursors **18** and cyclic pentamers **6**. Anthracene units in **6** are marked by **A–E**.

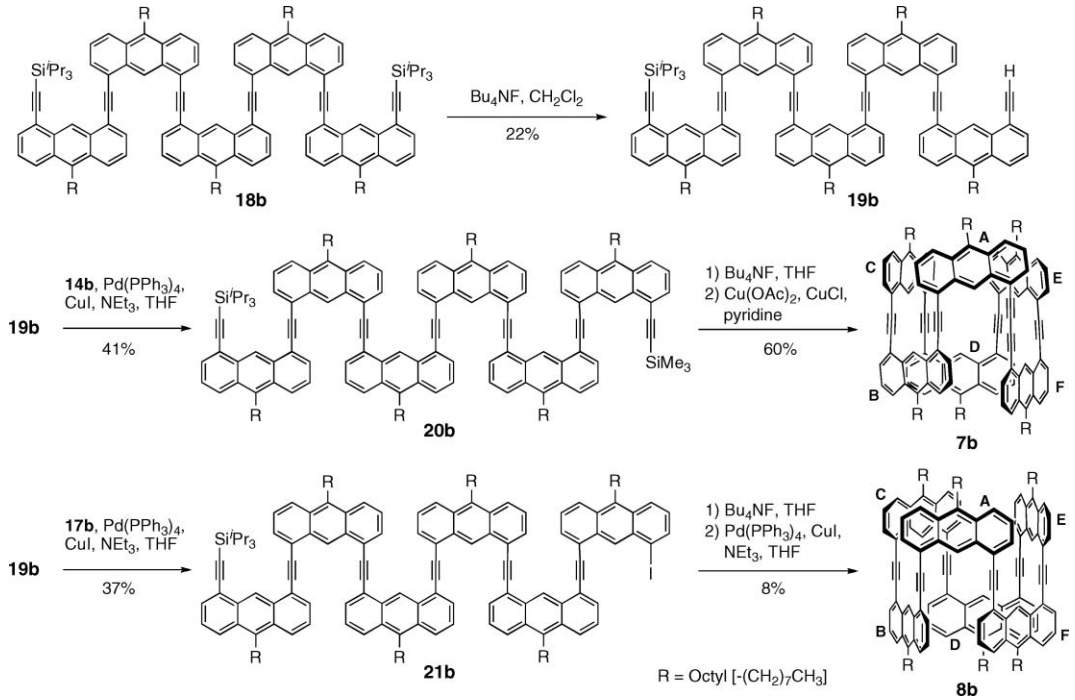

Scheme 2 Synthesis of cyclic hexamers **7b** and **8b**. Anthracene units in **7b** and **8b** are marked by **A–F**.

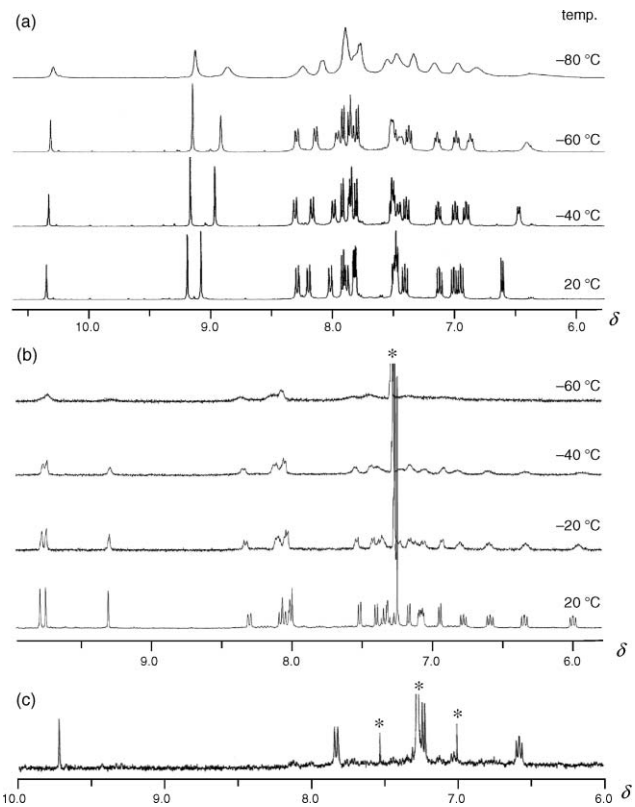

Fig. 3 ^{1}H NMR spectra of cyclic oligomers in the aromatic region. (a) VT NMR of **6b** in CD_2Cl_2, (b) VT NMR of **7b** in $CDCl_3$, and (c) NMR of **8b** at room temperature in $CDCl_3$. * Signals due to $CHCl_3$ and its ^{13}C satellites.

of **6b** appeared at a high magnetic field (δ 6.6–7.0) and one singlet due to the 10-H proton of anthracene **C** appeared at a low magnetic field (δ 10.4). These shifts could be understood from the ring current effect of the anthracene moieties in the cyclic structure.

In the case of chiral hexamer **7b**, six sets of ABC systems and three singlets (1 : 1 : 1 intensity) were observed in the aromatic region of the ^{1}H NMR spectrum [Fig. 3(b)], and seven alkynic carbon signals were seen in the ^{13}C NMR spectrum. These signal patterns can be explained by the C_2 symmetric structure. The ^{1}H NMR signals became considerably simpler upon macrocyclization of **21b** to form **8b**, which gave one set of ABC system, one singlet, and one set of alkyl signals [Fig. 3(c)]. Unfortunately, we could not measure the ^{13}C NMR spectra of **8b** because of its low solubility.

The chemical shifts of the alkyne carbons in **6b** and **7b** are compared with those of other cyclic oligomers, strain-free cyclic tetramers **1** and **2** and strained cyclic trimer **4**, in Table 1.[4,5] While the signals of diacetylene carbons were usually observed at δ *ca.* 80, one of the signals of **6b** (δ 88.2) was apparently shifted to the low magnetic field. As for acetylene carbons, two signals of **6b** were slightly shifted in the same direction. These deshielding effects can be attributed to the bending deformations of alkynic carbons, as generally observed for strained alkynes[3a,18,19] such as

Table 1 ^{13}C NMR chemical shifts of acetylene carbons of cyclic pentamer **6b** and cyclic hexamer **7b** and related compounds[a]

Compound	^{13}C NMR/δ	
	–C≡C–C≡C–	–C≡C–
6b	81.6, 88.2	93.3, 94.8, 95.3, 96.9
7b	79.7, 81.3	92.6, 93.1, 93.4, 94.57, 94.62
1	—	93.1
2	80.1, 81.1	—
4	82.4, 89.1	94.8, 96.1

[a] Measured in $CDCl_3$ at room temperature.

those involved in **4**.[6] The chemical shifts of **7b** are comparable to those of strain-free reference compounds, showing insignificant bending deformation. These data are discussed later on the basis of molecular structures.

Electronic spectra

The UV–vis and fluorescence spectra of the cyclic oligomers are shown in Fig. 4. Absorption bands in the *p*-band region appeared in the range of 380–480 nm. Peaks at the longest wavelength were observed at *ca.* 460 nm, and were longer by *ca.* 10 nm than those of the corresponding acyclic precursors. The small effect of cyclization was also noted for the other oligomer systems such as tetramers and trimers.[5,6] In the fluorescence spectra, emission bands were observed as broad peaks at 500–510 nm. The fluorescence quantum yields Φ_f are 0.17, 0.13, and 0.07 for **6b–8b**, respectively. Upon cyclization, we observed small bathochromic shifts in the wavelengths with increased intensities for the emission peaks. The fluorescence quantum yields of the cyclic oligomers are smaller than those of **1** (0.40), **4** (0.24), and **5** (0.39).[4,6,7] The effective fluorescence quenching as well as the broadening of emission bands of the hexamers are attributable to intramolecular π···π contacts in the folded cyclic frameworks because this phenomenon is occasionally observed for π systems such as cyclophanes and in the solid state.[20,21]

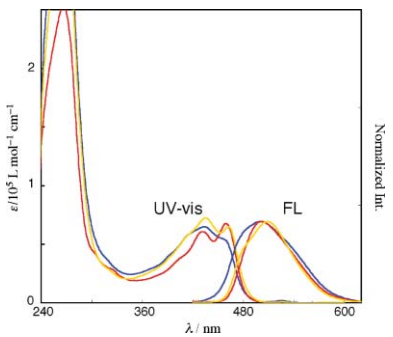

Fig. 4 UV–vis and fluorescence spectra of **6b** (red), **7b** (yellow), and **8b** (blue) in $CHCl_3$.

Molecular structure

As we could not obtain single crystals suitable for X-ray analysis, the molecular structures of the macrocyclic oligomers were examined by DFT calculations. We optimized the structures of alkyl-free compounds **6a–8a** from several initial structures at the M05/3-21G level (Fig. 5–7).[22] This calculation method was able to reproduce the structures of such macrocyclic oligomer systems within a reasonable computation time.[5,12] For example, the observed diamond-prism structure of **1** was obtained by this method, in contrast to the calculations by other methods, such as DFT calculation by conventional B3LYP functional and HF calculation with various basis sets.

Pentamer **6a** has two optimized structures **I** and **II**, both of which lack a plane of symmetry (Fig. 5). The framework of **I** is slightly twisted from the C_s symmetric structure, and this structure is much more stable than **II**. Anthracenes **B** and **D** are nearly parallel at the distance of 3.4–3.6 Å in **I**, while they are offset in **II**. Alkyne carbons, in particular diacetylene carbons, are significantly

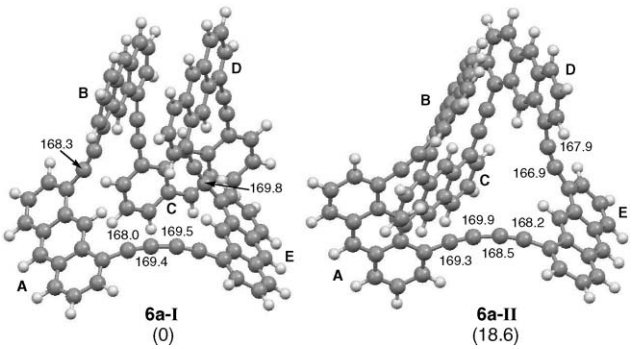

Fig. 5 Calculated structures of **6a** at the M05/3-21G level. Relative energies are in parentheses in kJ mol^{-1}. Bond angles of alkyne carbons are shown in degrees in cases where the value is less than 170°.

deformed from the linear geometry in both structures, and the bond angles of some carbons are less than 170°. These bending deformations are consistent with the deshielding of some alkyne carbons in the ^{13}C NMR spectrum as mentioned above.

Acyclic hexamer **8a** is regarded as a mechanical linkage with six links and six pins, which should have three degrees of freedom according to the geometrical theory. Structural optimization of achiral hexamer **8a** gave three structures (Fig. 6). The global minimum structure is a slightly deformed parallelogram prism of C_i symmetry (**P**), where the internal angles are *ca.* 143° and 37°. The second most stable structure is a triangular prism of D_3 symmetry (**T**). The rectangular prism structure of C_{2h} symmetry (**R**) is much less stable than the other two structures. The bond angles of alkyne carbons are in the range of 176–180° and the bending deformations are less significant than those in the pentamer. In structure **P**, there are two pairs of parallel oriented anthracene groups (**B**···**F** and **C**···**E**) separated by 3.6 Å, and some C–H···π contacts at 2.6–2.8 Å (**A**···**E**, **B**···**D**, and others). The triangular structure has several C–H···π contacts at 2.7–2.8 Å, but no face-to-face orientations of anthracene moieties. In the rectangular structure, the interlayer distance between anthracene planes is 5.2 Å, which is too large for transannular interactions. These structural features suggest that π···π interactions play an important role in the conformational preference, as also found in cyclic tetramers **1–3**.[4,5] Namely, anthracene units tend to stack in the oligomeric structures, and this trend is consistent with

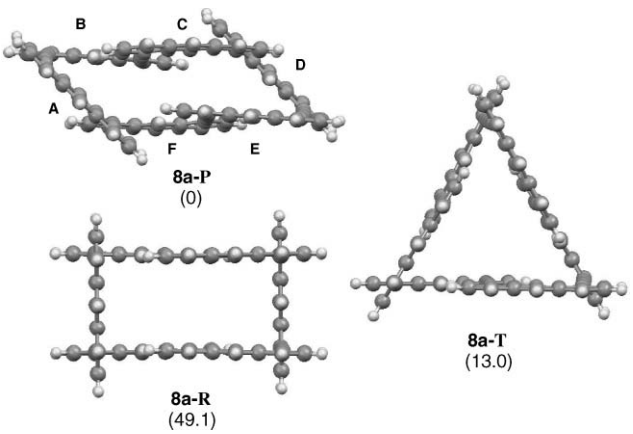

Fig. 6 Calculated structures of **8a** at the M05/3-21G level. Relative energies are in parentheses in kJ mol^{-1}.

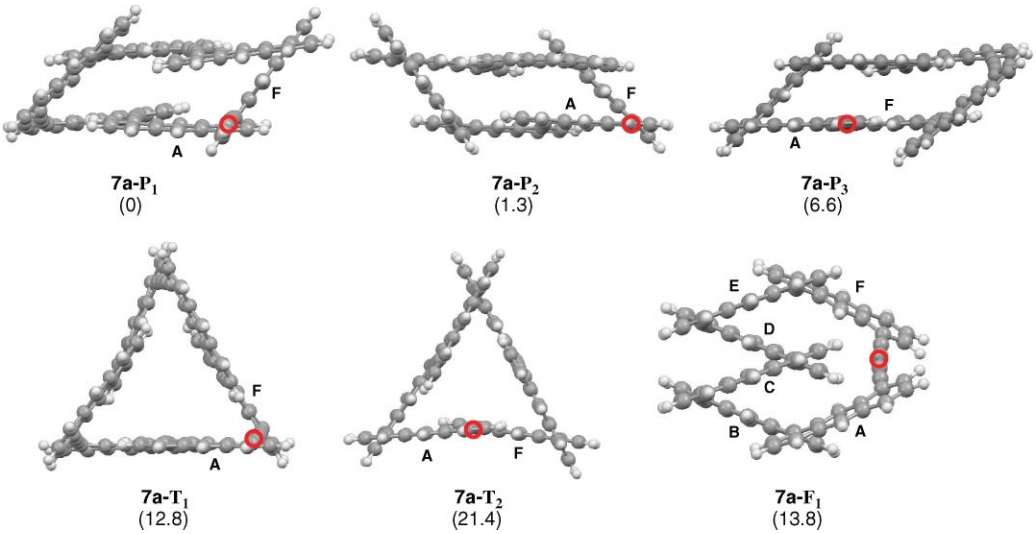

Fig. 7 Calculated structures of **7a** at the M05/3-21G level. Three less stable internally folded conformers are not shown here. Relative energies are in parentheses in kJ mol^{-1}. Diacetylene linkers connecting anthracenes **A** and **F** are marked with red circles.

the theoretical calculations of the anthracene dimer, giving large binding energies of up to 40 kJ mol^{-1}.[23]

The structures of chiral hexamer **7a** are discussed in a manner similar to those of the achiral hexamer except for the presence of one diacetylene linker. The optimized structures are classified into three groups, parallelogram, triangle, and internally folded structures, among which the parallelogram structures are the most stable (Fig. 7). There are three parallelogram structures $\mathbf{P_1}$–$\mathbf{P_3}$, where the diacetylene linker occupies the obtuse angle corner, the acute angle corner, and the midpoint of the longer side, respectively. The global minimum structure is $\mathbf{P_1}$ and the other two structures have comparable energies. The interlayer distances between the parallel oriented anthracenes are 3.4–3.5 Å in those structures. As regards the triangular structures, $\mathbf{T_1}$ with the diacetylene linker at the corner is more stable than $\mathbf{T_2}$ with this at the midpoint of the side. We obtained four internally folded-prism structures upon optimization with the diacetylene linkers at various positions, among which the most stable one is shown in Fig. 7. The other three structures are less stable by >26 kJ mol^{-1} than the global minimum structure, and their populations should be practically zero under ordinary conditions. There are two pairs of triply parallel anthracenes in $\mathbf{F_1}$ (**A**···**C**···**E**, **B**···**D**···**F**), although the structure seems to be sterically congested. The calculated relative energies indicate that most of the actual molecules exist in one of the parallelogram structures. The preference for the parallelogram structures is also attributable to the π···π interactions in the cyclic structures.

Dynamic behavior

The ^{1}H NMR spectra of the cyclic oligomers were measured at low temperature to explore the dynamic behavior of the macrocyclic framework in solution. The observed spectra in the aromatic region are shown in Fig. 3.

The ^{1}H NMR spectrum of pentamer **6b** is consistent with C_s symmetry at room temperature and even at –60 °C in CD_2Cl_2, contrary to the calculated less symmetric structure **I** in Fig. 5. This observation means that the interconversion between **I** and its enantiomeric form should take place rapidly on the NMR timescale at –60 °C. This dynamic process led to exchanges between anthracenes **A** and **E** (**B** and **D**). All the proton signals became broad at low temperatures because of the restricted rotation of the octyl groups, as reported for other 10-alkyl substituted oligomers.[4,16] Primary alkyl groups at this position preferred the bisected conformation relative to the anthracene plane, and the two bisected conformations of each octyl group in the cyclic system resulted in diastereomeric forms.

The proton signals of chiral hexamer **7b** became slightly broad at –20 °C and very broad at –60 °C in $CDCl_3$. We were unable to measure its spectra at lower temperature in CD_2Cl_2 or other solvents because of its low solubility. This broadening can be explained by the slow exchanges between the parallelogram conformations, although it is not straightforward to differentiate the restricted rotation of the octyl groups separately. The stable calculated structures all take parallelogram conformations $\mathbf{P_1}$–$\mathbf{P_3}$ of C_1 symmetry. Therefore, the conformational interconversions that change the position of the diacetylene linker take place rapidly at room temperature to afford the C_2 symmetric NMR spectra. This motion is similar to the rolling of a caterpillar belt, although we could not obtain sufficient information on the conformation of the transition state from available data. We could not measure the ^{1}H NMR spectra of **8b** at low temperature because of its very low solubility. The highly symmetric signal pattern at room temperature suggests facile exchanges between possible parallelogram and triangular structures: namely, the molecules of **8b** are conformationally fluxional *via* facile rotation of anthrylene units about acetylene linkers.[24]

Enantiomeric resolution of cyclic hexamer 7b

Because cyclic hexamer **7b** has a chiral belt-shaped structure, we resolved its enantiomers by chiral HPLC. We used a Daicel CHIRALPAK® IA column because it is known for excellent performance in the resolution of various compounds[25] containing anthracene oligomers.[5,12,26] The enantiomers were eluted at 25.1 and 30.9 min with hexane–chloroform (10 : 1) with almost baseline

separation. The specific rotations of the first and second fractions were $[\alpha]_D^{20}$ +206 and −215, respectively. The CD spectra of these enantiomers are mirror images of each other, although their intensities are not strong (Fig. 8). The more easily eluted (+)-isomer gave a sharp trough at 276 nm, continuous peaks at 290–330 nm, and broad peaks in the range of 420–480 nm. The Cotton effects in the longest wavelength region corresponded to the *p*-band absorption in the UV–vis spectrum.

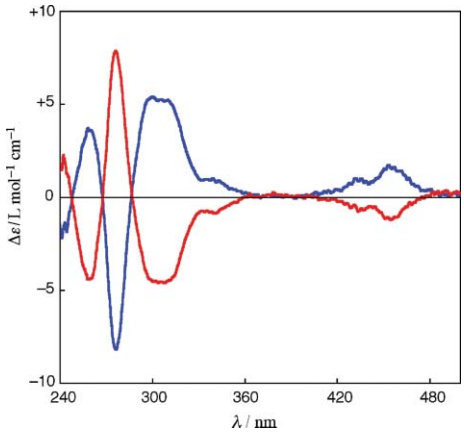

Fig. 8 CD spectra of enantiomers of **7b** in $CHCl_3$. Blue: easily eluted (+)-isomer. Red: less easily eluted (−)-isomer.

The stereochemistry of these enantiomers could be specified by the helicity of the two anthracene groups about the diacetylene linker, *P* (plus) or *M* (minus), as shown in Fig. 9. We could not predict the absolute stereochemistry from available data because experimental and theoretical approaches were obstructed by the large size of molecule. When an enantiopure sample of **7b** was heated at 125 °C in octane for 24 h, the compound mostly decomposed without racemization. This experiment indicated that the racemization was negligibly slow at a high temperature and the barrier should be higher than 144 kJ mol^{-1}. The belt-shaped molecule must mutually change the inside and the outside after racemization *via* highly strained structures as the transition state.

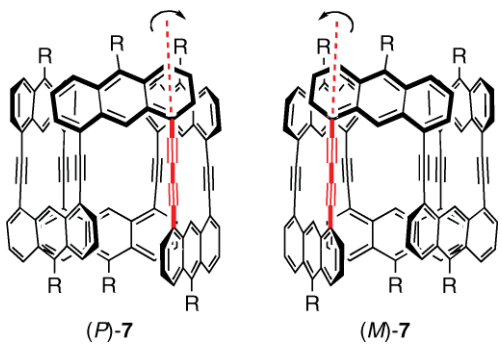

Fig. 9 Enantiomers of chiral cyclic hexamer **7** and their stereochemical descriptions.

Conclusion

We synthesized three types of anthracene–acetylene macrocyclic oligomers by means of coupling reactions. Whereas pentamers **6** have strained and rather rigid structures, hexamers **7** and **8** are almost strain-free and conformationally flexible. The hexamers prefer to take parallelogram-prism conformations due to stabilization by π···π interactions. The enantiomers of chiral hexamer **7b** were successfully resolved by chiral HPLC to give novel enantiopure belt-shaped molecules. The ability to synthesize macrocyclic compounds containing up to 44-membered rings should promise the formation of larger cyclic frameworks. If we can control the conformational distributions of such macrocyclic compounds, the nature of their variable shapes will be applicable to the development of functional molecules. This can be achieved by, for example, controlling photophysical properties, interactions with external molecules, and the folding mode. Further studies are in progress.

Experimental

General

Melting points are uncorrected. Elemental analyses were performed by a Perkin-Elmer 2400 series analyzer. NMR spectra were measured on a Varian Gemini-300 (^{1}H: 300 MHz, ^{13}C: 75 MHz), a JEOL GSX-400 (^{1}H: 400 MHz, ^{13}C: 100 MHz), or a JEOL Lambda-500 (^{1}H: 500 MHz, ^{13}C: 125 MHz) spectrometer. ^{1}H NMR spectra at low temperature were measured on a JEOL GSX-400 spectrometer at 400 MHz. The temperature was calibrated with the chemical shift differences of signals of methanol. High-resolution FAB mass spectra were measured on a JEOL MStation-700 spectrometer. MALDI-TOF mass spectra were measured on a Voyager-Biocad spectrometer. UV spectra were measured on a Hitachi U-3000 spectrometer with a 10 mm cell. Fluorescence spectra were measured on a JASCO FP-6500 spectrofluorometer with a 10 mm cell at room temperature. Column chromatography was carried out with Merck Silica Gel 60 (70–230 mesh) or Fuji Silysia Chromatorex-NH (100–200 mesh). In the ^{1}H-NMR data, the signals are assignable to anthracene protons unless otherwise noted. Analytical and spectroscopic data of intermediate or by-products and ^{13}C NMR data of **19b–21b** are given in the Supporting Information‡.

Synthesis and characterization

Acyclic pentamer 18a. A solution of **16a**[12] (51 mg, 0.087 mmol) and **17a**[13] (17 mg, 0.040 mmol) in THF (23 mL) and triethylamine (23 mL) was degassed by Ar gas for 15 min, and $Pd(PPh_3)_4$ (4.6 mg, 4.0 μmol), and CuI (0.83 mg, 4.4 μmol) were added to the solution. The reaction mixture was refluxed for 66 h under Ar. After the solvent was evaporated, the crude products were purified by chromatography on silica gel with hexane–dichloromethane (5 : 1) as eluent. The product was recrystallized from benzene to give pure material as yellow solid (43 mg, 80%). Mp 281–282 °C; δ_H (500 MHz, $CDCl_3$) 0.33 (6H, septet, *J* 7.6, ^{i}Pr), 0.58 (36H, d, *J* 7.6, ^{i}Pr), 6.38–6.44 (4H, m), 6.76 (2H, dd, *J* 7.1, 8.6), 6.98 (2H, d, *J* 6.7), 7.20–7.30 (12H, m), 7.53 (2H, d, *J* 8.6), 7.57 (4H, d, *J* 6.7), 7.78–7.82 (5H, m), 7.94 (2H, s), 8.05 (2H, s), 9.08 (2H, s), 9.12 (1H, s), 9.57 (2H, s); δ_C (125 MHz, $CDCl_3$) 11.18, 18.25, 92.50, 92.82, 92.90, 96.22, 104.82, 120.80, 121.08, 121.60, 121.76, 122.08, 123.50, 123.64, 123.86, 124.23, 124.28, 124.31, 124.36, 124.53, 125.91, 126.47, 126.82, 127.60, 127.69, 127.75, 128.37, 128.69, 128.97, 129.50, 129.56, 130.04, 130.11, 130.42, 130.59,

130.71, 130.75, 130.84, 130.97, 131.24, 131.38 (one alkyl and two aromatic signals are missing); UV ($CHCl_3$) λ_{max} (ε) 248 (335000), 414 (57800), 437 (50600) nm; FL ($CHCl_3$) λ_{max} 482 nm, λ_{ex} 393 nm (Φ_f 0.047); MS (MALDI-TOF) Found m/z 1338.75. Calcd for $C_{100}H_{82}Si_2$: M^+, m/z 1338.60; Anal. Found: C, 89.26; H, 6.28%. Calcd for $C_{100}H_{82}Si_2$: C, 89.64; H, 6.17%.

Cyclic pentamer 6a. To a solution of **18a** (50 mg, 37.3 μmol) in THF (30 mL) was added a TBAF solution (1.0 mol L^{-1} in THF, 74.6 μL, 74.6 μmol). After the solution was stirred for 30 min at room temperature, the solvent was evaporated. The residue was used for the next reaction without further purification and NMR measurement because of its very poor solubility. The residue was suspended in pyridine (75 mL), and $Cu(OAc)_2 \cdot H_2O$ (186 mg, 0.93 mmol) and CuCl (74 mg, 0.75 mmol) were added. The reaction mixture was stirred for 19 h at room temperature. After the solvent was evaporated, the residual solid was submitted to chromatography on silica gel (NH) with hexane–chloroform (2 : 1) as eluent. The desired compound was obtained as a yellow solid (6.6 mg, 17%). Mp 348–360 °C (dec); δ_H (500 MHz, CD_2Cl_2) 6.80 (2H, d, J 7.4), 6.97 (2H, t, J 6.7), 7.04 (2H, t, J 7.3), 7.11 (2H, t, J 7.4), 7.33 (2H, d, J 8.6), 7.45 (2H, t, J 7.0), 7.50 (2H, d, J 7.7), 7.57 (2H, d, J 6.4), 7.69 (2H, d, J 8.3), 7.79–7.81 (4H, m), 7.88 (2H, d, J 7.0), 7.92–7.94 (4H, m), 7.99 (2H, d, J 7.7), 8.03 (2H, d, J 9.2), 8.36 (2H, s), 8.48 (1H, s), 9.04 (2H, s), 9.25 (2H, s), 10.23 (1H, s); UV ($CHCl_3$) λ_{max} (ε) 258 (236000), 420 (51900), 446 (54200) nm; FL ($CHCl_3$) λ_{max} 494 nm, λ_{ex} 393 nm (Φ_f 0.27); HRMS (FAB) Found m/z 1024.3130. Calcd for $C_{82}H_{40}$: M^+, m/z 1024.3148.

1,8-Dichloro-10-octylanthracene (10b). To a mixture of Mg (831 mg, 34.2 mmol) in ether (5 mL) was added a solution of 1-bromooctane (6.0 mL, 34 mmol) in ether (12 mL) over 90 min under Ar. The mixture was stirred for 90 min. After the solution was diluted with ether (100 mL), 4,5-dichloro-9-anthrone (**9**)[15] (3.00 g, 11.4 mmol) was added. The reaction mixture was stirred for 20 h at room temperature, and quenched with aq NH_4Cl. The products were extracted with ether, dried over $MgSO_4$, and evaporated. The crude product was purified by chromatography on silica gel with hexane as eluent to give a yellow solid (1.90 g, 46%). Mp 65–66 °C; δ_H (300 MH, $CDCl_3$) 0.89 (3H, t, J 6.3, octyl), 1.22–1.44 (8H, m, octyl), 1.56 (2H, m, octyl), 1.81 (2H, m, octyl), 3.57 (2H, t, J 8.7, octyl), 7.43 (2H, dd, J 7.2, 8.4), 7.62 (2H, d, J 7.2), 8.22 (2H, d, J 8.4), 9.26 (1H, s); δ_C (75 MHz, $CDCl_3$) 14.12, 22.65, 28.67, 29.30, 29.45, 30.23, 31.46, 31.87, 119.52, 123.60, 125.23, 125.44, 129.09, 130.39, 133.15, 137.04; HRMS (FAB) Found m/z 358.1261. Calcd for $C_{22}H_{24}{}^{35}Cl_2$: M^+, m/z 358.1255; Anal. Found: C, 73.73; H, 6.97%. Calcd for $C_{22}H_{24}Cl_2$: C, 73.54; H, 6.73%.

10-Octyl-1,8-bis[(trimethylsilyl)ethynyl]anthracene (11b). To a solution of (trimethylsilyl)ethyne (3.1 mL, 22.2 mmol) in THF (52 mL) was added an ethylmagnesium bromide solution (1.0 mol L^{-1} in ether, 20.0 mL, 20.0 mmol) at 0 °C under Ar. After this solution was stirred for 1 h, **10b** (2.00 g, 5.57 mmol), $Ni(acac)_2$ (100 mg, 0.39 mmol), PPh_3 (102 mg, 0.39 mmol) were added. The reaction mixture was refluxed for 48 h under Ar, and then quenched with aq NH_4Cl (*ca.* 30 mL). The organic layer was separated, dried over $MgSO_4$, and evaporated. The crude product was purified by chromatography on silica gel with hexane as eluent followed by recrystallization from ethanol to give a yellow solid (1.87 g, 69%). Mp 93–94 °C; δ_H (300 MHz, $CDCl_3$) 0.39 (18H, s, Me), 0.90 (3H, t, J 7.3, octyl), 1.29–1.39 (8H, m, octyl), 1.55 (2H, m, octyl), 1.76 (2H, quintet, J 7.8, octyl), 3.56 (2H, t, J 7.8, octyl), 7.44 (2H, dd, J 6.8, 8.8), 7.78 (2H, d, J 6.8), 8.25 (2H, d, J 8.8), 9.31 (1H, s); δ_C (75 MHz, $CDCl_3$) 0.53, 14.20, 22.74, 28.41, 29.38, 29.58, 30.33, 31.66, 31.94, 99.70, 103.94, 121.97, 122.64, 124.70, 125.52, 129.15, 131.02, 131.91, 136.66; HRMS (FAB) Found m/z 482.2777. Calcd for $C_{32}H_{42}Si_2$: M^+, m/z 482.2825; Anal. Found: C, 79.74; H, 8.98%. Calcd for $C_{32}H_{42}Si_2$: C, 79.60; H, 8.77%.

1,8-Diethynyl-10-octylanthracene (12b). A solution of **11b** (500 mg, 1.04 mmol) and KF (302 mg, 5.20 mmol) in EtOH (25 mL) was refluxed for 2 h. After the solvent was evaporated, the residue was dissolved in dichloromethane. The organic solution was washed with aq NaCl, dried over $MgSO_4$, and evaporated. The crude product was purified by chromatography on silica gel with hexane as eluent to give the desired compound as yellow solid (345 mg, 98%). Mp 60–61 °C; δ_H (300 MHz, $CDCl_3$) 0.87 (3H, t, J 6.3, octyl), 1.29 (8H, m, octyl), 1.49 (2H, quintet, J 7.3, octyl), 1.70 (2H, quintet, J 7.3, octyl), 3.46 (2H, t, J 7.3, octyl), 3.59 (2H, s, ≡C–H), 7.39 (2H, dd, J 6.8, 8.8), 7.74 (2H, d, J 6.8), 8.19 (2H, d, J 8.8), 9.40 (1H, s); δ_C (75 MHz, $CDCl_3$) 14.20, 22.73, 28.26, 29.37, 29.54, 30.31, 31.65, 31.93, 82.00, 82.56, 120.95, 122.46, 124.67, 125.73, 129.02, 130.98, 131.33, 136.74; HRMS (FAB) Found m/z 338.1998. Calcd for $C_{26}H_{26}$: M^+, m/z 338.2035; Anal. Found: C, 91.89; H, 8.04%. Calcd for $C_{26}H_{26}$: C, 92.26; H, 7.74%.

1 - Ethynyl - 10 - octyl - 8 - [(triisopropylsilyl) ethynyl] anthracene (13b). To a solution of **12b** (200 mg, 0.59 mmol) in dry THF (8 mL) was added a BuLi solution (1.56 mol L^{-1} in hexane, 0.42 mL, 0.65 mmol) at −78 °C under Ar. The solution was stirred for 90 min at that temperature, and then allowed to warm up to 0 °C. After chlorotriisopropylsilane (0.125 mL, 0.59 mmol) was added, the solution was stirred for 2 h at 0 °C and then for 17 h at room temperature. The reaction mixture was quenched with aq NH_4Cl, and the volatile materials were removed by evaporation. The residue was extracted with dichloromethane. The organic layer was separated, dried over $MgSO_4$, and evaporated. The crude product was purified by chromatography on silica gel with hexane as eluent. The desired compound was obtained as yellow oil (173 mg, 60%). The starting material (25 mg, 13%) was recovered. δ_H (300 MHz, $CDCl_3$) 0.91 (3H, m, ^{i}Pr), 1.12–1.40 (29H, m, ^{i}Pr and octyl), 1.56 (2H, m, octyl), 1.77 (2H, m, octyl), 3.51 (1H, s, ≡C–H), 3.56 (2H, t, J 7.8, octyl), 7.44–7.48 (2H, m), 7.79 (2H, d, J 6.8), 8.23–8.28 (2H, m), 9.48 (1H, s); δ_C (75 MHz, $CDCl_3$) 11.57, 14.20, 19.01, 22.74, 28.31, 29.38, 29.58, 30.32, 31.69, 31.95, 82.10, 82.49, 96.27, 105.33, 121.00, 122.39, 122.76, 124.60, 124.84, 125.27, 125.79, 129.05, 129.18, 131.17, 131.18, 131.37, 131.41, 136.70; HRMS (FAB) Found m/z 494.3346. Calcd for $C_{35}H_{46}Si$: M^+, m/z 494.3369.

Dimer 15b. A solution of **14b**[16] (160 mg, 0.321 mmol) in THF (6 mL) and triethylamine (6 mL) was degassed by Ar gas for 30 min, and $Pd(PPh_3)_4$ (18 mg, 16 μmol), and CuI (3.0 mg, 16 μmol) were added to the solution. To the solution was added a solution of **13b** (154 mg, 0.321 mmol) in THF (4 mL) and triethylamine (4 mL) was added in 5 h under reflux under H_2. The solution was further refluxed for 40 h. After the solvent was evaporated, the crude product was purified by chromatography on silica gel with hexane–dichloromethane (30 : 1) as eluent to give the desired compound as

yellow oil (269 mg, 95%). δ_H (400 MHz, $CDCl_3$) –0.31 (9H, s, Me), 0.65 (3H, septet, *J* 6.9, ^{i}Pr), 0.74 (18H, d, *J* 6.8, ^{i}Pr), 0.92–0.96 (6H, m, octyl), 1.34–1.48 (16H, m, octyl), 1.60 (4H, m, octyl), 1.84 (4H, m, octyl), 3.65 (4H, t, *J* 6.8, octyl), 7.47 (2H, m), 7.56 (2H, m), 7.73 (1H, d, *J* 6.8), 7.77 (1H, d, *J* 6.8), 7.95 (1H, d, *J* 6.4), 7.99 (1H, d, *J* 6.8), 8.29 (2H, d, *J* 8.8), 8.35 (2H, dd, *J* 2.4, 9.6), 9.62 (1H, s), 9.65 (1H, s); δ_C (100 MHz, $CDCl_3$) –0.63, 11.17, 18.45, 14.21, 22.76, 28.25, 28.32, 29.42, 29.67, 30.25, 30.26, 30.34, 31.71, 31.74, 31.99, 92.61, 92.70, 96.58, 99.98, 103.10, 105.22, 122.27, 122.57, 122.64, 123.19, 123.35, 124.68, 124.71, 124.81, 125.11, 125.28, 125.31, 129.19, 129.23, 129.31, 129.37, 130.47, 130.61, 131.01, 131.04, 131.41, 131.47, 131.50, 131.54, 136.40, 136.45 (4 alkyl and 3 aromatic signals missing); HRMS (FAB) Found *m*/*z* 878.5626. Calcd for $C_{62}H_{78}Si_2$: M^+, *m*/*z* 878.5642.

Dimer 16b. A solution of **15b** (138 mg, 0.16 mmol) and KF (46 mg, 0.78 mmol) in EtOH (25 mL) was refluxed for 2.5 h. After the solvent was evaporated, the residue was dissolve in dichloromethane. The organic solution was washed with aq NaCl, dried over $MgSO_4$, and evaporated. The crude product was purified by chromatography on silica gel with hexane–dichloromethane (30 : 1) as eluent to give the desired compound as a yellow solid (119 mg, 94%). Mp 178–179 °C; δ_H (300 MHz, $CDCl_3$) 0.65 (3H, septet, *J* 7.2, ^{i}Pr), 0.76 (18H, d, *J* 7.2, ^{i}Pr), 0.82–0.92 (6H, m, octyl), 1.23–1.43 (16H, m, octyl), 1.59 (4H, quintet, *J* 7.1, octyl), 1.82 (4H, quintet, *J* 7.7, octyl), 2.90 (1H, s, ≡C–H), 3.59–3.64 (4H, m, octyl), 7.41–7.47 (2H, m), 7.50–7.57 (2H, m), 7.69 (1H, d, *J* 6.4), 7.75 (1H, d, *J* 6.4), 7.90 (1H, d, *J* 7.1), 7.99 (1H, d, *J* 6.4), 8.25–8.35 (4H, m), 9.66 (1H, s), 9.69 (1H, s); δ_C (75 MHz, $CDCl_3$) 11.25, 14.10, 18.40, 22.68, 28.31, 28.40, 29.35, 29.57, 30.33, 31.68, 31.72, 31.91, 81.71, 82.68, 93.08, 93.62, 96.77, 105.29, 121.48, 122.65, 122.73, 122.80, 123.36, 124.74, 124.94, 125.00, 125.20, 125.33, 125.43, 125.67, 129.25, 129.34, 129.43, 129.97, 130.65, 130.92, 131.42, 131.54, 131.65, 131.79, 136.66, 136.70 (6 alkyl and 4 aromatic peaks missing); HRMS (FAB) Found *m*/*z* 806.5235. Calcd for $C_{59}H_{70}Si$: M^+, *m*/*z* 806.5247; Anal. Found: C, 87.43; H, 8.61%. Calcd for $C_{59}H_{70}Si$: C, 87.78; H, 8.74%.

Acyclic pentamer 18b. A solution of **17b**[16] (123 mg, 0.226 mmol) in THF (6 mL) and triethylamine (6 mL) was degassed by Ar gas for 30 min, to which $Pd(PPh_3)_4$ (26 mg, 22 μmol), and CuI (4.2 mg, 22 μmol) were added. To the solution was added a solution of **16b** (364 mg, 0.451 mmol) in THF (4 mL) and triethylamine (4 mL) was added in 5 h under reflux under H_2 atmosphere. The solution was further refluxed for 72 h. After the volatile materials were evaporated, the crude products were purified by chromatography on silica gel with hexane–chloroform (10 : 1) as eluent. The product was recrystallized from benzene to give pure material as yellow solid (266 mg, 62%). Mp 173.5–174.5 °C (dec); δ_H (400 MHz, $CDCl_3$) 0.31–0.43 (6H, m, ^{i}Pr), 0.59 (36H, d, *J* 7.3, ^{i}Pr), 0.92–0.98 (15H, m, octyl), 1.20–1.85 (60H, m, octyl), 3.26 (2H, m, octyl), 3.41–3.55 (8H, m, octyl), 6.15 (2H, t, *J* 7.4), 6.61 (2H, t, *J* 7.6), 6.82 (2H, t, *J* 7.8), 7.00 (2H, d, *J* 6.3), 7.19–7.23 (2H, m), 7.28–7.37 (6H, m), 7.54 (2H, d, *J* 8.8), 7.63 (4H, d, *J* 6.3), 7.78 (2H, d, *J* 8.8), 7.92 (2H, d, *J* 8.8), 8.02 (2H, d, *J* 8.8), 8.10 (2H, d, *J* 8.8), 9.31 (1H, s), 9.43 (2H, s), 9.77 (2H, s); δ_C (100 MHz, $CDCl_3$) 11.25, 14.25, 18.37, 22.82, 28.29, 28.42, 28.49, 29.48, 29.51, 29.53, 29.69, 29.77, 30.44, 30.47, 30.59, 31.52, 31.71, 31.75, 32.02, 32.05, 92.96, 93.02, 93.09, 93.40, 96.54, 105.26, 121.94, 121.99, 122.45, 122.65, 122.79, 122.92, 123.55, 123.82, 124.02, 124.38, 124.43, 124.51, 124.56, 124.84, 128.14, 128.60, 128.77, 128.86, 128.91, 129.00, 129.45, 129.53, 130.13, 130.74, 130.88, 130.98, 131.04, 131.08, 131.27, 134.39, 135.27, 135.59 (6 alkyl and 4 aromatic signals missing); UV ($CHCl_3$) λ_{max} (ε) 268 (275000), 404 (42800), 427 (54200), 452 (44900) nm; FL ($CHCl_3$) λ_{max} 466, 489 nm, λ_{ex} 393 nm (Φ_f 0.09); Anal. Found: C, 88.13; H, 8.38%. Calcd for $C_{140}H_{162}Si_2$: C, 88.46; H, 8.59%.

Cyclic pentamer 6b. To a solution of **18b** (50 mg, 26 μmol) in THF (20 mL) was added a TBAF solution (1.0 mol L^{-1} in THF, 53 μL, 53 μmol). After the solution was stirred for 3 h at room temperature, the solvent was evaporated. Thus formed terminal alkyne was used for the next reaction without further purification. An analytical sample was obtained by chromatography on silica gel with hexane–chloroform (4 : 1) as eluent. The crude terminal alkyne was dissolved in pyridine (24 mL). To the solution were added $Cu(OAc)_2 \cdot H_2O$ (132 mg, 0.66 mmol) and CuCl (52 mg, 0.53 mmol). After the reaction mixture was stirred for 1 h at room temperature, the solvent was evaporated. The crude product was purified by chromatography on silica gel (NH) with hexane–chloroform (4 : 1) as eluent. The desired compound was obtained as a yellow solid (25 mg, 60%). Mp 61–62 °C (dec); δ_H (500 MHz, $CDCl_3$) 0.75–1.70 (75H, m, octyl), 3.13–3.28 (2H, br, octyl), 3.30–3.44 (2H, br, octyl), 3.43–3.46 (4H, m, octyl), 3.54–3.57 (2H, m, octyl), 6.58 (2H, d, *J* 7.1), 6.93–6.96 (2H, m), 6.99 (2H, dd, *J* 6.7, 8.9), 7.16 (2H, dd, *J* 7.1, 8.9), 7.39 (2H, dd, *J* 7.0, 8.9), 7.44 (2H, d, *J* 8.9), 7.47–7.51 (4H, m), 7.80–7.84 (4H, m), 7.86 (2H, d, *J* 6.7), 7.90 (2H, d, *J* 6.7), 7.97 (2H, d, *J* 8.9), 8.15 (2H, d, *J* 8.9), 8.25 (2H, d, *J* 8.9), 9.10 (2H, s), 9.22 (2H, s), 10.39 (1H, s); δ_C (125 MHz, $CDCl_3$) 14.03, 14.10, 14.12, 22.58, 22.63, 22.66, 28.18, 28.27, 29.23, 29.28, 29.31, 29.46, 29.47, 29.49, 29.70, 30.15, 30.22, 30.24, 31.54, 31.60, 31.64, 31.84, 31.86, 31.91, 81.59, 88.24, 93.34, 94.78, 95.26, 96.87, 121.55, 121.64, 122.69, 122.82, 122.97, 123.04, 123.14, 123.84, 124.10, 124.17, 124.28, 124.51, 124.56, 124.71, 124.91, 125.14, 125.33, 125.95, 128.29, 128.41, 128.84, 129.29, 129.43, 129.64, 129.69, 130.32, 130.41, 130.88, 131.39, 132.40, 132.50, 134.88, 136.24, 136.70 (2 aromatic signals missing); UV ($CHCl_3$) λ_{max} (ε) 266 (20700), 431 (48800), 459 (53300) nm; FL ($CHCl_3$) λ_{max} 509 nm, λ_{ex} 393 nm (Φ_f 0.17); HRMS (FAB) Found *m*/*z* 1584.9438. Calcd for $C_{122}H_{120}$: M^+, *m*/*z* 1584.9390.

Pentamer 19b. To a solution of **18b** (342 mg, 0.18 mmol) in dichloromethane (130 mL) was added a TBAF solution (1.0 mol L^{-1} in THF, 0.180 mL, 0.18 mmol). After the solution was stirred for 2 h at room temperature, water (30 mL) was added. The organic layer was separated, dried over $MgSO_4$, and evaporated. The crude products were separated by chromatography on silica gel with hexane–chloroform (10 : 1) as eluent. The desired product (second fraction) was obtained as a yellow solid (69 mg, 22%). The starting material (the first fraction) and the fully desilylated product (the third fraction) were obtained in 51 and 16%, respectively, and the latter was identical with the terminal alkyne obtained during the synthesis of **6b**. Mp 179–180 °C (dec); δ_H (400 MHz, $CDCl_3$) 0.56 (3H, septet, *J* 7.2, ^{i}Pr), 0.68 (18H, d, *J* 7.2, ^{i}Pr), 0.90–0.95 (15H, m, octyl), 1.46–1.83 (60H, m, octyl), 2.70 (1H, s, ≡C–H), 3.19 (2H, t, *J* 8.8, octyl), 3.24 (2H, t, *J* 8.8, octyl), 3.42 (2H, t, *J* 6.8, octyl), 3.49 (2H, t, *J* 8.8, octyl), 3.57 (2H, t, *J* 8.8, octyl), 5.99 (1H, dd, *J* 7.1, 9.2), 6.35 (1H, dd, *J* 7.1, 9.2), 6.54 (1H, dd, *J* 7.1, 9.2), 6.64–6.71 (2H, m), 6.87–6.99 (3H, m), 7.06–7.20 (4H, m), 7.26–7.60 (13H, m), 7.67 (2H, d, *J* 7.1), 7.74

(2H, dd, *J* 3.6, 9.2), 7.81 (2H, d, *J* 7.1), 8.00 (2H, dd, *J* 5.0, 8.6), 8.18 (2H, t, *J* 9.2), 9.29 (1H, s), 9.46 (1H, s), 9.52 (1H, s), 9.60 (1H, s), 9.90 (1H, s); HRMS (FAB) Found *m/z* 1743.0870. Calcd for $C_{131}H_{142}Si$: M^+, *m/z* 1743.0081.

Hexamer 20b. A solution of **19b** (100 mg, 57 μmol) and **14b** (88 mg, 172 μmol) in THF (4 mL) and triethylamine (4 mL) was purged by H_2 gas, and $Pd(PPh_3)_4$ (21 mg, 17 μmol) and CuI (1.1 mg, 5.7 μmol) were added to the solution. After the reaction mixture was refluxed for 42 h under H_2, the solvent was evaporated. The crude product was purified by chromatography on silica gel with hexane–chloroform (5 : 1) as eluent. The desired compound was obtained as a yellow solid (50 mg, 41%). Mp 206–207 °C (dec); δ_H (500 MHz, $CDCl_3$) –0.12 (9H, s, Me), 0.49 (3H, septet, *J* 7.2, ^{i}Pr), 0.62 (18H, d, *J* 7.2, ^{i}Pr), 0.88–0.96 (18H, m, octyl), 1.25–1.85 (72H, m, octyl), 3.17 (2H, t, *J* 7.8, octyl), 3.23 (2H, t, *J* 7.8, octyl), 3.29 (2H, t, *J* 8.2, octyl), 3.39–3.43 (4H, m, octyl), 3.61 (2H, t, *J* 8.3, octyl), 5.87 (1H, dd, *J* 6.7, 8.9), 6.20–6.24 (2H, m), 6.36 (1H, dd, *J* 6.7, 8.9), 6.43 (1H, dd, *J* 6.7, 8.9), 6.75 (2H, t, *J* 7.8), 6.83–6.89 (2H, m), 6.91 (1H, d, *J* 7.0), 6.94 (1H, d, *J* 6.4), 7.04 (1H, dd, *J* 6.7, 8.9), 7.10 (1H, d, *J* 6.4), 7.20 (1H, d, *J* 6.7), 7.24 (1H, dd, *J* 7.0, 8.8), 7.29–7.34 (2H, m), 7.36–7.49 (4H, m), 7.55 (2H, t, *J* 9.9), 7.61–7.71 (6H, m), 7.74 (1H, d, *J* 6.4), 7.80 (1H, d, *J* 6.4), 7.92 (1H, d, *J* 9.5), 8.06–8.09 (2H, m), 8.11 (1H, d, *J* 9.2), 8.22 (1H, d, *J* 9.2), 9.23 (1H, s), 9.35 (1H, s), 9.53 (1H, s), 9.62 (1H, s), 9.65 (1H, s), 9.66 (1H, s); UV ($CHCl_3$) λ_{max} (ε) 268 (271000), 405 (42200), 427 (52800), 453 (43200) nm; FL ($CHCl_3$) λ_{max} 494 nm, λ_{ex} 393 nm (Φ_f 0.06); MS (MALDI-TOF) Found *m/z* 2127.28. Calcd for $C_{158}H_{174}Si_2$: M^+, *m/z* 2127.31.

Chiral cyclic hexamer 7b. To a solution of **20b** (50 mg, 24 μmol) in THF (20 mL) was added a TBAF solution (1.0 mol L^{-1} in THF, 48 μL, 48 μmol). After the solution was stirred for 10 min at room temperature, the solvent was evaporated. Thus formed terminal alkyne was used for the next reaction without further purification. An analytical sample was obtained by chromatography on silica gel with hexane–chloroform (4 : 1) as eluent. The crude terminal alkyne was dissolved in pyridine (35 mL). To the solution were added $Cu(OAc)_2{\cdot}H_2O$ (117 mg, 0.56 mmol) and CuCl (47 mg, 0.47 mmol). After the reaction mixture was stirred for 17 h at room temperature, the solvent was evaporated. The crude product was purified by chromatography on silica gel (NH) with hexane–chloroform (4 : 1) as eluent to give the desired compound as a yellow solid (27 mg, 60%). Mp 157–158 °C (dec); δ_H (400 MHz, $CDCl_3$) 0.88–1.09 (18H, m, octyl), 1.25–1.56 (62H, m, octyl), 1.65–1.74 (6H, m, octyl), 1.84–1.97 (4H, m, octyl), 2.76–2.90 (4H, m, octyl), 3.60 (4H, t, *J* 8.8, octyl), 3.70 (4H, t, *J* 8.6, octyl), 6.00 (2H, dd, *J* 6.8, 8.8), 6.35 (2H, dd, *J* 6.8, 8.8), 6.59 (2H, dd, *J* 6.8, 8.8), 6.78 (2H, dd, *J* 7.2, 8.4), 6.95 (2H, d, *J* 6.8), 7.07–7.11 (4H, m), 7.17 (2H, d, *J* 6.8), 7.31–7.38 (6H, m), 7.41 (2H, d, *J* 6.8), 7.53 (2H, d, *J* 6.8), 8.02 (4H, d, *J* 7.2), 8.08 (4H, t, *J* 8.2), 8.31 (2H, d, *J* 8.4), 9.32 (2H, s), 9.77 (2H, s), 9.81 (2H, s); δ_C (100 MHz, $CDCl_3$) 14.21, 17.87, 18.13, 22.79, 28.11, 28.42, 28.48, 29.40, 29.53, 29.57, 29.70, 29.80, 30.36, 30.57, 31.29, 31.82, 32.04, 79.62, 81.23, 92.54, 92.98, 93.29, 94.47, 94.53, 120.83, 121.79, 122.13, 122.24, 122.38, 123.36, 123.43, 123.67, 123.72, 123.93, 124.11, 124.45, 124.60, 124.61, 124.82, 124.89, 125.41, 125.88, 128.39, 128.48, 128.83, 129.06, 129.18, 129.48, 129.86, 130.19, 130.83, 130.88, 130.94, 131.00, 131.03, 131.12, 131.21, 131.48, 134.97, 135.54, 136.05 (7 alkyl and 5 aromatic signals missing); UV ($CHCl_3$) λ_{max} (ε) 268 (285000), 435 (57900), 462 (52100) nm; FL ($CHCl_3$) λ_{max} 502 nm, λ_{ex} 393 nm (Φ_f 0.13); HRMS (FAB) Found *m/z* 1897.1283. Calcd for $C_{146}H_{144}$: M^+, *m/z* 1897.1268.

Hexamer 21b. A solution of **19b** (100 mg, 57 μmol) and **17b** (155 mg, 287 μmol) in THF (4 mL) and triethylamine (4 mL) was purged by H_2, and $Pd(PPh_3)_4$ (33 mg, 29 μmol) and CuI (5.5 mg, 29 μmol) were added to the solution. After the reaction mixture was refluxed for 42 h under H_2, the solvent was evaporated. The crude product was purified by chromatography on silica gel with hexane–chloroform (4 : 1) as eluent. The desired compound was obtained as a yellow solid (45 mg, 37%). A small amount of 11-mer was obtained as a by-product (*ca.* 12%). Mp 85–86 °C; δ_H (500 MHz, $CDCl_3$) 0.50 (3H, septet, *J* 7.2, ^{i}Pr), 0.63 (18H, d, *J* 7.0, ^{i}Pr), 0.86–0.98 (18H, m, octyl), 1.25–1.79 (70H, m, octyl), 1.90 (2H, quintet, *J* 7.9, octyl), 3.17–3.26 (6H, m, octyl), 3.34 (2H, t, *J* 7.9, octyl), 3.44 (2H, t, *J* 7.9, octyl), 3.69 (2H, t, *J* 7.9, octyl), 5.83 (1H, dd, *J* 6.7, 8.9), 6.19 (1H, dd, *J* 7.0, 8.9), 6.28–6.34 (2H, m), 6.52 (1H, dd, *J* 6.7, 8.9), 6.64–6.72 (4H, m), 6.84 (1H, d, *J* 6.7), 6.93–7.03 (4H, m), 7.14–7.19 (2H, m), 7.41–7.50 (6H, m), 7.55–7.58 (3H, m), 7.62 (1H, d, *J* 9.2), 7.70 (1H, d, *J* 6.4), 7.76 (1H, d, *J* 6.4), 7.80 (1H, d, *J* 9.2), 7.84 (1H, d, *J* 6.7), 7.89 (1H, d, *J* 6.7), 7.96 (1H, d, *J* 6.7), 7.99 (1H, d, *J* 8.9), 8.19 (1H, d, *J* 8.9), 8.22 (1H, d, *J* 9.2), 8.29 (1H, d, *J* 9.2), 9.02 (1H, s), 9.25 (1H, s), 9.64 (1H, s), 9.65 (1H, s), 9.68 (1H, s), 9.78 (1H, s); UV ($CHCl_3$) λ_{max} (ε) 268 (269000), 406 (42000), 428 (50900), 453 (39900) nm; FL ($CHCl_3$) λ_{max} 493 nm, λ_{ex} 393 nm (Φ_f 0.03); MS (MALDI-TOF) Found *m/z* 2157.38. Calcd for $C_{153}H_{165}ISi$: M^+, *m/z* 2157.17.

Achiral cyclic hexamer 8b. To a solution of **21b** (37 mg, 20 μmol) in THF (20 mL) was added a TBAF solution (1.0 mol L^{-1} in THF, 20 μL, 20 μmol). After the solution was stirred for 10 min at room temperature, the solvent was evaporated. Thus formed terminal alkyne was used for the next reaction without further purification. An analytical sample was obtained by chromatography on silica gel with hexane–chloroform (2 : 1) as eluent. The terminal alkyne was dissolved in THF (20 mL) and NEt_3 (20 mL). To the solution were added $Pd(PPh_3)_4$ (6.8 mg, 5.9 μmol) and CuI (1.1 mg, 5.9 μmol) under H_2. After the reaction mixture was refluxed for 20 h at room temperature, the solvent was evaporated. The crude product was purified by chromatography on silica gel (NH) with hexane–chloroform (4 : 1) as eluent to give the desired compound as a yellow solid (3.0 mg, 8%). Mp 130–131 °C (dec); δ_H (400 MHz, $CDCl_3$) 0.80–2.18 (90H, m, octyl), 3.45 (12H, m, octyl), 6.59 (12H, t, *J* 8.6), 7.20 (12H, d, *J* 8.6), 7.81 (12H, d, *J* 8.6), 9.71 (6H, s); UV ($CHCl_3$) λ_{max} (ε) 267 (293000), 434 (52000), 456 (43600, sh) nm; FL ($CHCl_3$) λ_{max} 500 nm, λ_{ex} 393 nm (Φ_f 0.07); HRMS (FAB) Found *m/z* 1873.1233. Calcd for $C_{144}H_{144}$: M^+, *m/z* 1873.1268.

DFT calculation

The calculations were carried out with Gaussian 03W[27] on a Windows computer. The structures were optimized by hybrid DFT at the M05/3-21G level from several input structures.

Enantiomeric resolution

Optical rotations were measured on a JASCO DIP-370 digital polarimeter with a 3.5ϕ × 100 mm cell. CD spectra were measured on a JASCO J-820 polarimeter with a 10 mm cylindrical cell.

Enantiomers of **7b** were resolved with a Daicel CHIRALPAK® IA column (10 mmϕ × 250 mm) with hexane–chloroform (10 : 1) as eluent. A solution of racemic **7b** (*ca.* 1.5 mg) in chloroform (1.5 mL) was injected for each batch with flow rate of 2.0 mL min^{-1}. Enantiomers were eluted at 25.1 and 50.9 min under the conditions. First fraction: $[\alpha]_D^{20}$ +206 (*c* 0.065, $CHCl_3$); CD ($CHCl_3$): λ ($\Delta\varepsilon$) 258 (+3.7), 276 (–8.2), 306 (+5.3), 436 (+1.0), 453 nm (+1.7). Second fraction: $[\alpha]_D^{20}$ –215 (*c* 0.075, $CHCl_3$); CD ($CHCl_3$): λ ($\Delta\varepsilon$) 258 (–4.4), 276 (+7.9), 308 (–4.4), 434 (–0.7), 455 nm (–1.2).

Acknowledgements

This work was partly supported by Grants-in-Aid for Scientific Research (C) No. 19550054 and for Scientific Research on Innovative Areas (Integrated Organic Synthesis) No. 22106543 from MEXT (Ministry of Education, Culture, Sports, Science and Technology, Japan) and by matching fund subsidy for private universities from MEXT. The authors thank Dr M. Goichi, Ms. Y. Okagawa, and Mr. M. Sasaki for technical assistance, and Associate Prof. K. Wakamatsu for helpful discussion in computational chemistry.

Notes and references

1 K. Miyamoto, T. Iwanaga and S. Toyota, *Chem. Lett.*, 2010, **39**, 288–290.
2 *Poly(arylene ethynylene)s*, ed. by C. Weder, Springer, Heidelberg, 2005.
3 (*a*) T. Kawase, *Synlett*, 2007, 2609–2626; (*b*) E. L. Spitler, C. A. Johnson, II and M. M. Haley, *Chem. Rev.*, 2006, **106**, 5344–5386; (*c*) W. Zhang and J. S. Moore, *Angew. Chem., Int. Ed.*, 2006, **45**, 4416–4439; (*d*) D. Zhao and J. S. Moore, *Chem. Commun.*, 2003, 807–818; (*e*) Y. Tobe, N. Utsumi, K. Kawabata, A. Nagano, K. Adachi, S. Araki, M. Sonoda, K. Hirose and K. Naemura, *J. Am. Chem. Soc.*, 2002, **124**, 5350–5364; (*f*) S. Höger, *Chem.–Eur. J.*, 2004, **10**, 1320–1329.
4 (*a*) S. Toyota, M. Goichi and M. Kotani, *Angew. Chem., Int. Ed.*, 2004, **43**, 2248–2251; (*b*) S. Toyota, M. Goichi, M. Kotani and M. Takezaki, *Bull. Chem. Soc. Jpn.*, 2005, **78**, 2214–2227.
5 S. Toyota, H. Miyahara, M. Goichi, S. Yamasaki and T. Iwanaga, *Bull. Chem. Soc. Jpn.*, 2009, **82**, 931–945.
6 S. Toyota, H. Miyahara, M. Goichi, K. Wakamatsu and T. Iwanaga, *Bull. Chem. Soc. Jpn.*, 2008, **81**, 1147–1157.
7 S. Toyota, M. Kurokawa, M. Araki, K. Nakamura and T. Iwanaga, *Org. Lett.*, 2007, **9**, 3655–3658.
8 (*a*) H. Meier, in *Carbon-Rich Compounds*, ed. M. M. Haley and R. R. Tykwinski, Wiley-VCH, Wienheim, 2006, chap. 11; (*b*) T. M. Swager, in *Acetylene Chemistry*, ed. F. Diederich, P. J. Stang and R. R. Tykwinski, Wiley-VCH, Weinheim, 2005, chap. 6.
9 (*a*) R. Herges, in *Modern Cyclophane Chemistry*, ed. R. Gleiter and H. Hopf, Wiley-VCH, Weinheim, 2004, chap. 13; (*b*) R. Herges, *Chem. Rev.*, 2006, **106**, 4820–4842; (*c*) R. Jasti, J. Bhattacharjee, J. B. Neaton and C. R. Betozzi, *J. Am. Chem. Soc.*, 2008, **130**, 17646–17647; (*d*) H. Takaba, H. Omachi, Y. Yamamoto, J. Bouffard and K. Itami, *Angew. Chem., Int. Ed.*, 2009, **48**, 6112–6116.
10 (*a*) P. Kissel, A. D. Schlüter and J. Sakamoto, *Chem.–Eur. J.*, 2009, **15**, 8955–8960; (*b*) P. Kissel, J. van Heijst, R. Enning, A. Stemmer, A. D. Schlüter and J. Sakamoto, *Org. Lett.*, 2010, **12**, 2778–2781.
11 (*a*) K. Campbell and R. R. Tykwinski, in *Carbon-Rich Compounds*, ed. M. M. Haley and R. R. Tykwinski, Wiley-VCH, Weinheim, 2006, chap. 6; (*b*) R. Herges, M. Deichmann, T. Wakita and Y. Okamoto, *Angew. Chem., Int. Ed.*, 2003, **42**, 1170–1172.
12 (*a*) T. Ishikawa, T. Shimasaki, H. Akashi and S. Toyota, *Org. Lett.*, 2008, **10**, 417–420; (*b*) T. Ishikawa, T. Shimasaki, H. Akashi, T. Iwanaga, S. Toyota and M. Yamasaki, *Bull. Chem. Soc. Jpn.*, 2010, **83**, 220–232.
13 M. Goichi, K. Segawa, S. Suzuki and S. Toyota, *Synthesis*, 2005, (13), 2116–2118.
14 P. Siemsen, R. C. Livingston and F. Diederich, *Angew. Chem., Int. Ed.*, 2000, **39**, 2632–2657.
15 H. O. House, J. A. Hrabie and D. VanDerveer, *J. Org. Chem.*, 1986, **51**, 921–929.
16 S. Toyota, S. Suzuki and M. Goichi, *Chem.–Eur. J.*, 2006, **12**, 2482–2487.
17 A. Elangovan, Y.-H. Wang and T.-I. Ho, *Org. Lett.*, 2003, **5**, 1841–1844.
18 G. Gleiter and R. Merger, in *Modern Acetylene Chemistry*, ed. P. J. Stang and F. Diederich, VCH, Weinheim, 1995, chap. 8.
19 E. Breitmaier and W. Voelter, *Carbon-13 NMR Spectroscopy*, VCH, New York, 1995, chap. 4.3.
20 (*a*) W.-L. Wang, J. Xu, Z. Sun, X. Zhang, Y. Lu and Y.-H. Lai, *Macromolecules*, 2006, **39**, 7277–7285; (*b*) Y. Morisaki, T. Murakami, T. Sawamura and Y. Chujo, *Macromolecules*, 2009, **42**, 3656–3660; (*c*) P. Rademacher, in *Modern Cyclophane Chemistry*, ed. R. Gleiter and H. Hopf, Wiley-VCH, Weinheim, 2004, chap. 11; (*d*) Y. Liu, X. Tao, F. Wang, X. Dang, D. Zou, Y. Ren and M. Jiang, *Org. Electron.*, 2009, **10**, 1082–1090.
21 Mechanisms of fluorescence quenching. (*a*) B. Valeur, *Molecular Fluorescence*, Wiley-VCH, Weinheim, 2002, chap. 4; (*b*) J. R. Lakowicz, *Principles of Fluorescence Spectroscopy*, 3rd Ed., New York, 2006, chap. 8.
22 (*a*) Y. Zhao, N. E. Schultz and D. G. Truhlar, *J. Chem. Theory Comput.*, 2006, **2**, 364–382; (*b*) Y. Zhao and D. G. Truhlar, *J. Phys. Chem. A*, 2006, **110**, 10478–10486; (*c*) Y. Zhao and D. G. Truhlar, *Acc. Chem. Res.*, 2008, **41**, 157–167.
23 (*a*) C. Gonzalez and E. C. Lim, *J. Phys. Chem. A*, 2000, **104**, 2953–2957; (*b*) C. Gonzalez and E. C. Lim, *J. Phys. Chem. A*, 2003, **107**, 10105–10110.
24 S. Toyota, *Chem. Rev.* Articles ASAP 10.1021/cr1000628.
25 T. Ikai and Y. Okamoto, *Chem. Rev.*, 2009, **109**, 6077–6101.
26 S. Toyota, H. Onishi, K. Wakamatsu and T. Iwanaga, *Chem. Lett.*, 2009, **38**, 350–351.
27 *Gaussian 03, Revision E.01*, M. J. Frisch, G. W. Trucks, H. B. Schlegel, G. E. Scuseria, M. A. Robb, J. R. Cheeseman, J. A. Montgomery, Jr., T. Vreven, K. N. Kudin, J. C. Burant, J. M. Millam, S. S. Iyengar, J. Tomasi, V. Barone, B. Mennucci, M. Cossi, G. Scalmani, N. Rega, G. A. Petersson, H. Nakatsuji, M. Hada, M. Ehara, K. Toyota, R. Fukuda, J. Hasegawa, M. Ishida, T. Nakajima, Y. Honda, O. Kitao, H. Nakai, M. Klene, X. Li, J. E. Knox, H. P. Hratchian, J. B. Cross, V. Bakken, C. Adamo, J. Jaramillo, R. Gomperts, R. E. Stratmann, O. Yazyev, A. J. Austin, R. Cammi, C. Pomelli, J. W. Ochterski, P. Y. Ayala, K. Morokuma, G. A. Voth, P. Salvador, J. J. Dannenberg, V. G. Zakrzewski, S. Dapprich, A. D. Daniels, M. C. Strain, O. Farkas, D. K. Malick, A. D. Rabuck, K. Raghavachari, J. B. Foresman, J. V. Ortiz, Q. Cui, A. G. Baboul, S. Clifford, J. Cioslowski, B. B. Stefanov, G. Liu, A. Liashenko, P. Piskorz, I. Komaromi, R. L. Martin, D. J. Fox, T. Keith, M. A. Al-Laham, C. Y. Peng, A. Nanayakkara, M. Challacombe, P. M. W. Gill, B. Johnson, W. Chen, M. W. Wong, C. Gonzalez and J. A. Pople, Gaussian, Inc., Wallingford CT, 2004.

